7th International Conference on Contact Mechanics and Wear of Rail/Wheel Systems (CM2006), Brisbane, Australia, September 24-26, 2006

SPECIAL CLASS OF CONTACT PROBLEMS AND THE CALCULATION OF THE STATE OF STRESS OF WHEEL/RAIL SYSTEM ELEMENTS

L.A. Sosnovskiy*, S.S. Sherbakov#.

*Scientific and Production Group TRIBOFATIGUE Ltd., Gomel, Belarus
#Belarusian State University, Minsk, Belarus

*sosnovskiy@tribo-fatigue.com

ABSTRACT

A special class of contact problems arises if the combined state of stress of the active system elements in contact is governed both by the field of contact stresses and the field of stresses that is caused by volume loads (bending, tension - compression, torsion, etc.). The main principles of solving such problems are given in this work.

An active roller/ring system may to a certain extent serve as a model of a wheel/rail system. It is due to the fact that there is not only contact interaction in the wheel/rail system but also bending of the rail. The method of investigation of the state of stress of elements of such systems in the conditions of both static (accompanied by bending) and rolling (dynamic) contact is presented in the work. Numerical solution for the state of stress of the roller and ring is given. It shows that in some areas bending leads to the change of the sign of stresses. Their absolute values in some points change by hundred percent.

1 INTRODUCTION

In the mechanics of a deformable solid contact problems are a special wide field of research (see for example [1]). Special approach to statement and the solution of contact problems is developed in tribo-fatigue [2-5] as contact interaction of specific objects - active systems of machines and the equipment is studied.

Considering these systems the complex analysis is required both of surface deformation and damage in the local area of contact of two elements of a system and volume deformation and damage by effective load which causes various types of general deformation (bending, torsion, tension - compression, their combinations, etc.) of at least one of the elements of a system.

Table 1. Schemes of roller/roller and roller/ring contact

Element 1: $R_{11}>0$ $R_{12}>0$ Element 2: $R_{21}>0$ $R_{22}>0$	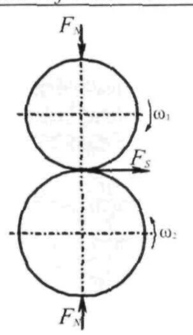	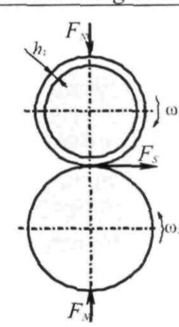
Contact type	*A*	*B*

General classification of contact problems for active systems of machines is offered in work [3]. Table 1 represents the part, which covers classification of contact problems for bodies of rotation. Here R_{11}, R_{12}, R_{21} and R_{22} are radii of curvature. Contact of type *B* corresponds to the simplest mechanical model for a wheel/rail system; it is designed for complex wear-fatigue tests by SI-series machines [2] (Fig. 1). Here the roller (element 2) simulates a wheel and the ring (element 1) simulates a rail. Below this model is named a roller/ring system.

Principal particularity of the roller/ring system in comparison with the corresponding traditional contact problem for the roller/roller model (tab. 1, type *A*) is that the full state of stress of the ring in the zone of its interaction with the roller is caused not only by the field of contact stresses but also by the field of stresses caused by bending.

The method of investigation of the state of stress of the roller/ring system is stated in the paper.

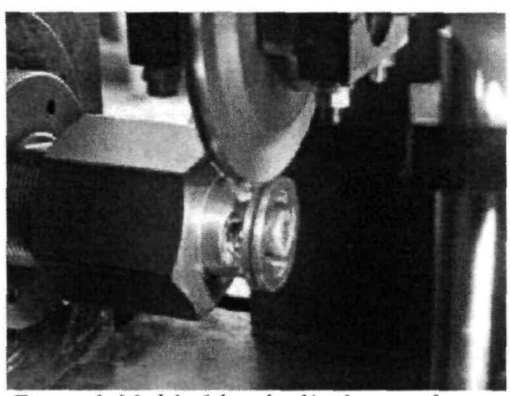

Figure 1. Model of the wheel/rail system for complex wear-fatigue tests

2 MAIN PROVISIONS

1) Force F_N acting in the considered active system generally causes both local deformation of a roller and a ring in the neighborhood of the point of initial contact and deformation (bending) of the ring as a whole. In order to study the state of stress of the system we will assume that in the contact area F_N it is divided into contact F_c and bending F_b components under the following condition

$$F_N=F_c+F_b. \tag{1}$$

Let us consider a condition of energy balance of a solid as the equality of energy of deformation and work performed by surface forces along corresponding displacements if volumetrically distributed loads are absent in the solid:

$$\iiint_V T\cdot\cdot E dV + \iint_S \overline{F}\overline{u} dS = 0 \tag{2}$$

where $T\cdot\cdot E$ – biscalar product of tensors of stresses T and strains E, $\overline{F}$ – surface forces, $\overline{u}$ – surface displacements.

In order to define the values of F_c and F_b let us record the following general system of equations which takes into account the division of forces (1) and the condition of energy balance (2):

$$\begin{cases} \iiint_V T\cdot\cdot E dV + F_N u_N = 0, \\ F_c + F_b = F_N. \end{cases} \tag{3}$$

here T and E generally are also functions of F_c and F_b.

2) Let us consider a more simple way of determination of values F_c and F_b offered in works [3,4]. The ratio between components F_c and F_b of contact load F_b generally depends on volume rigidity of the ring EI_z/l (E – modulus of elasticity of ring material, I_z – moment of inertia of cross-section, l – length of the arch of the bar from the point of contact load application to the nearest support) or on the ratio between the determining sizes of the bar h/l accurate within a constant k. The constant k hence reflects mainly the influence of rigidity of a material on the formation of components F_c and F_b.

3) It is assumed that division of components F_c and F_b is described by exponential law

$$F_c = F_N\left(1-\exp\left(-\frac{h}{lk}\right)\right), \quad F_b = F_N \exp\left(-\frac{h}{lk}\right) \tag{4}$$

with condition (3) being satisfied. The law (4) is considered correct in the interval

$$0 \le \frac{h}{lk} \le \infty. \tag{5}$$

When $l \to \infty$, the case $h/lk = 0$ means that a curved bar is transformed into the bar of infinite length for which $F_N = F_b$ and $F_c = 0$. When $l \to 0$, the case $h/lk = \infty$ means that the ring is transformed into the roller (or curved bar into the half of the roller) for which $F_N = F_c$ and $F_b = 0$;

4) By virtue of particularities of geometry of investigated interacting bodies of finite sizes ($R_{11}>0$, $R_{12}>0$ for the roller and $R_{21}>0$, $R_{22}>0$ for the ring – see. Tab. 1) area of their contact will always be an ellipse (with big a and small b semi-axes).

5) The form and the area of the ellipse of contact in the investigated system is additionally determined by the change of the main curvature of a ring owing to its bending, i.e.

$$k_{21} = \frac{1}{R_{21}} - \frac{1}{\rho_M}, \tag{6}$$

where ρ_M – change of the radius of curvature caused by bending of the ring axis.

3 CONTACT AREA PARAMETERS

We will calculate parameters of the surface of contact with the account of the given assumptions under set geometry of the roller and the ring and applied load: sizes of semi-axes of the ellipse a, b and the maximum pressure p_0 in the center of the surface of contact.

Generally in order to calculate parameters of elliptic surface of contact geometrical parameter Ω [1,6]:

$$\Omega = \frac{1}{\sum k}\sqrt{(k_{11}-k_{12})^2 + (k_{21}-k_{22})^2 + 2(k_{11}-k_{12})(k_{21}-k_{22})\cos 2\gamma} \tag{7}$$

and eccentricity of an ellipse of contact e are determined first:

$$\begin{aligned} e^2(\Omega) &= e(\Omega(R_{11}(t), R_{12}(t), R_{21}(t), R_{22}(t), \theta(t))) = \\ &= 2{,}667\Omega - 3{,}577\Omega^2 + 4{,}244\Omega^3 - 5{,}871\Omega^4 + \\ &+ 10{,}312\Omega^5 - 18{,}202\Omega^6 + 24{,}577\Omega^7 - \\ &- 21{,}858\Omega^8 + 11{,}213\Omega^9 - 2{,}506\Omega^{10}. \end{aligned} \tag{8}$$

where k_{ij} ($ij = 1,2$) – curvatures of contacting bodies:

$$k_{11} = \frac{1}{R_{11}}, \quad k_{12} = \frac{1}{R_{12}}, \quad k_{21} = \frac{1}{R_{21}} - \frac{1}{\rho_M}, \quad k_{22} = \frac{1}{R_{22}},$$

$$\sum k = k_{11} + k_{12} + k_{21} + k_{22}.$$

Formulae [1,6] for determination of semi-axes of the ellipse a, b, magnitude of ellipse surface S, maximum pressure p_0 in the center of the surface of contact, compression δ under action of contact load F_c are

$$a = n_a\sqrt[3]{\frac{3}{2}\frac{\eta F_c}{\sum k}}, \quad b = n_b\sqrt[3]{\frac{3}{2}\frac{\eta F_c}{\sum k}}, \quad S = \pi ab,$$

$$p_0 = n_p\frac{1}{\pi}\sqrt[3]{\frac{3}{2}\left(\frac{\sum k}{\eta}\right)^2 F_c}, \tag{9}$$

$$\delta = n_\delta\frac{1}{2}\sqrt[3]{\frac{9}{4}\eta^2\sum k F_c^2},$$

here coefficients

$$n_a = \sqrt[3]{\frac{2}{\pi}\left(1+\frac{1-\Omega}{1+\Omega}\right)D(e)},\ n_p = \frac{1}{n_a n_b},$$

$$n_b = \sqrt[3]{\frac{2}{\pi}\left(1+\frac{1-\Omega}{1+\Omega}\right)(K(e)-D(e))\sqrt{1-e^2}}, \tag{10}$$

$$n_\delta = K(e)\sqrt[3]{\frac{4}{\pi^2}\frac{1}{\left(1+\frac{1-\Omega}{1+\Omega}\right)D(e)}},.$$

generalized parameter of properties of materials

$$\eta = \frac{1-\nu_1}{E_1} + \frac{1-\nu_2}{E_2} \tag{11}$$

and elliptic integrals

$$K(e) = \int_0^{\frac{\pi}{2}} \frac{d\varphi}{\sqrt{1-e^2\sin^2\varphi}},\ L(e) = \int_0^{\frac{\pi}{2}} \sqrt{1-e^2\sin^2\varphi}\,d\varphi,$$

$$D(e) = \frac{1}{e^2}\left[K(e) - L(e)\right]. \tag{12}$$

4 STATE OF STRESS

The state of stress in any point $M(\xi,\eta,z)$ of the system is determined from a general expression

$$\sigma_{ij}(\xi,\eta,z) = \sigma_{ij}^{(n)}(\xi,\eta,z) + \sigma_{ij}^{(\tau)}(\xi,\eta,z) + \sigma_{ij}^{(b)}(\xi,\eta,z), \tag{13}$$

where $\sigma_{ij}^{(n)}$ – stresses caused by normal contact traction, $\sigma_{ij}^{(\tau)}$ – stresses caused by tangential contact traction, $\sigma_{ij}^{(b)}$ – stresses caused by bending load.

Usually the study of the state of stress in the zone of contact in exact statement is limited to determination of stress tensor components in the points of the z-axis and in some points of the contact surface [6]. Determination of all the components of stress tensor in any point on the half-space in exact statement is problematic due to the extreme complexity of functions to integrate.

A non-conforming movable contact takes place between elements of active systems in which process of rolling friction is realized. In this case contact surface is the ellipse with elliptically distributed contact pressure $p(x,y)$ (Fig. 2). Since contact is movable, the state of stress is described by superposition of the stresses caused by normal $\sigma_{ij}^{(n)}$ $(i,j = x,y,z)$ and tangential $\sigma_{ij}^{(\tau)}$ contact tractions.

$$\sigma_{ij} = \sigma_{ij}^{(n)} + \sigma_{ij}^{(\tau)} \tag{14}$$

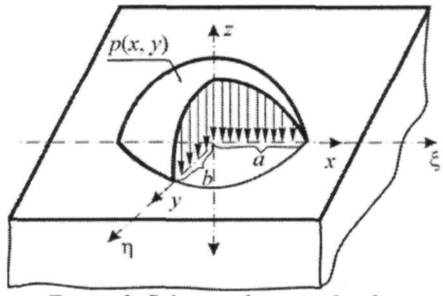

Figure 2. Scheme of contact loading

4.1 Surface Stresses Caused by Contact Pressure

Considering the solution of the given problem it is necessary to take into account that in different areas of contact zone (on the surface inside contact area, on its contour, beyond its boundaries, in the half-space under the surface) different relationships are applied to calculate the stresses [1,6].

Calculation of stresses in any point $M(\xi,\eta,0)$ on the surface under the action of elliptically distributed pressure is carried out according to the following general formula.

$$\sigma_{ij}^{(surf)}(\xi,\eta,0) = \sigma_{ij}^{(S)}(\xi,\eta), \tag{15}$$

where $\sigma_{ij}^{(S)}(\xi,\eta)$ – stresses on the surface of the half-space caused by pressure distributed over the area S: $\frac{x^2}{a^2}+\frac{y^2}{b^2} \le 1$.

Explicit form of expressions (15) is the following:

$$\frac{\sigma_{xx}^{(surf)}}{p_0} = \begin{cases} 2\nu - (1-2\nu)\dfrac{b}{a+b}\sqrt{1-\dfrac{x^2}{a^2}-\dfrac{y^2}{b^2}}, \\ \text{if } \dfrac{x^2}{a^2}+\dfrac{y^2}{b^2} < 1, \\ 0, \text{ if } \dfrac{x^2}{a^2}+\dfrac{y^2}{b^2} > 1, \end{cases} \tag{16}$$

$$\frac{\sigma_{yy}^{(surf)}}{p_0} = \begin{cases} -2\nu - (1-2\nu)\dfrac{a}{a+b}\sqrt{1-\dfrac{x^2}{a^2}-\dfrac{y^2}{b^2}}, \\ \text{if } \dfrac{x^2}{a^2}+\dfrac{y^2}{b^2} < 1, \\ 0, \text{ if } \dfrac{x^2}{a^2}+\dfrac{y^2}{b^2} > 1, \end{cases}$$

$$\frac{\sigma_{zz}^{(surf)}}{p_0} = \begin{cases} \sqrt{1-\dfrac{x^2}{a^2}-\dfrac{y^2}{b^2}}, \text{ if } \dfrac{x^2}{a^2}+\dfrac{y^2}{b^2} < 1, \\ 0, \text{ if } \dfrac{x^2}{a^2}+\dfrac{y^2}{b^2} > 1, \end{cases}$$

$$\frac{\sigma_{xy}^{(surf)}}{p_0} = \begin{cases} -(1-2\nu)\dfrac{b}{ae^2}\left[\dfrac{y}{ae}arth\left(\dfrac{ex}{a}\right) - \right. \\ \left. -\dfrac{x}{ae}arctg\left(\dfrac{aey}{b^2}\right)\right] = H(x,y), \text{ if } H(x,y)<0, \\ 0, \text{ if } H(x,y)>0, \end{cases}$$

$$\frac{\sigma_{xz}^{(surf)}}{p_0} = \frac{\sigma_{yx}^{(surf)}}{p_0} 0 .$$

Thus, formula (14) with the account of (15) is the following:

$$\sigma_{ij} = \sigma_{ij}^{(n)} + \sigma_{ij}^{(\tau)} = \left[\sigma_{ij}^{(hs)} \cup \sigma_{ij}^{(surf)}\right] + \sigma_{ij}^{(\tau)} . \quad (17)$$

4.2 Stresses Caused by Contact Pressure in a Half-space

Calculation of stresses $\sigma_{ij}^{(hs)}$ in any point of the half-space under the surface when $z<0$ under the action of elliptically distributed pressure (Fig. 2) is carried out numerically taking advantage of the Boussinesq problem solution $\sigma_{ij}^{(B)}$ [1,6] used to determine stress components in the half-space caused by unit normal force:

$$\sigma_{ij}^{(hs)}(\xi,\eta,z) = \iint\limits_{S(x,y)} p(x,y)\sigma_{ij}^{(B)}(x-\xi, y-\eta, z)dxdy . \quad (18)$$

Explicit form of expressions (18) is the following [4, 5, 6]:

$$\sigma_{xx}^{(hs)} = \iint\limits_S \frac{p_0\sqrt{1-\frac{x^2}{a^2}-\frac{y^2}{b^2}}}{2\pi}\left\{\frac{(1-2\nu)}{r^2}\left[\left(1-\frac{z}{\rho}\right)\frac{(x-\xi)^2-(y-\eta)^2}{r^2} + \right.\right.$$
$$\left.\left. + \frac{z(y-\eta)^2}{\rho^3}\right] - \frac{3z(x-\xi)^2}{\rho^5}\right\}dxdy,$$

$$\sigma_{yy}^{(hs)} = \iint\limits_S \frac{p_0\sqrt{1-\frac{x^2}{a^2}-\frac{y^2}{b^2}}}{2\pi}\left\{\frac{(1-2\nu)}{r^2}\left[\left(1-\frac{z}{\rho}\right)\frac{(y-\eta)^2-(x-\xi)^2}{r^2} + \right.\right.$$
$$\left.\left. + \frac{z(x-\xi)^2}{\rho^3}\right] - \frac{3z(y-\eta)^2}{\rho^5}\right\}dxdy,$$

$$\sigma_{zz}^{(hs)} = -\iint\limits_S \frac{3p_0\sqrt{1-\frac{x^2}{a^2}-\frac{y^2}{b^2}}}{2\pi}\frac{z^3}{\rho^5}dxdy, \quad (19)$$

$$\sigma_{xy}^{(hs)} = \iint\limits_S \frac{p_0\sqrt{1-\frac{x^2}{a^2}-\frac{y^2}{b^2}}}{2\pi}\left\{\frac{(1-2\nu)}{r^2}\left[\left(1-\frac{z}{\rho}\right)\frac{(x-\xi)(y-\eta)}{r^2} - \right.\right.$$
$$\left.\left. - \frac{(x-\xi)(y-\eta)z}{\rho^3}\right] - \frac{3(x-\xi)(y-\eta)z}{\rho^5}\right\}dxdy,$$

$$\sigma_{xz}^{(hs)} = -\iint\limits_S \frac{3p_0\sqrt{1-\frac{x^2}{a^2}-\frac{y^2}{b^2}}}{2\pi}\frac{(x-\xi)z^2}{\rho^5}dxdy,$$

$$\sigma_{yx}^{(hs)} = -\iint\limits_S \frac{3p_0\sqrt{1-\frac{x^2}{a^2}-\frac{y^2}{b^2}}}{2\pi}\frac{(y-\eta)z^2}{\rho^5}dxdy,$$

where $r^2 = (x-\xi)^2 + (y-\eta)^2$,

$\rho^2 = (x-\xi)^2 + (y-\eta)^2 + z^2$, $\frac{x^2}{a^2} + \frac{y^2}{b^2} = 1$ – equation determining area S.

The field of stresses in the half-space in each of considered points $M(\xi,\eta,z)$ is obtained by calculating all double integrals (19). To perform such an evaluation we will apply the following procedure. First each of the given integrals is calculated over x using Simpson's formula under fixed y taken from S with the certain step. Basing on the obtained set of points we construct approximation function (polynomial obtained by least squares method or a piecewise cubic spline) integration of which gives the second integral over y.

Taking into account that the problem is axially symmetric, we will carry out the evaluation only in the 1/4-th of the studied area. So the evaluation will take place at points $M \in X \times Y \times Z$, $X = \{0, \xi_1..ta\}$, $Y = \{0, \eta_1..ta\}$ $Z = \{0, z_1..ta\}$, where t - a multiplier determining the sizes of researched area, a – greater semi-axis of the contact ellipse, n – quantity of points along one coordinate. The distance between the nearest points is $h = ta/n$. Calculation for a large amount of points should be performed to obtain sufficiently accurate picture of the contact stresses distribution. It is expedient for computational shortcut to apply interpolation in area between the points of the basic grid stress components values of which are obtained after performing the procedure described above. Each new point is evaluated in the middle of the segment connecting two already available points. Values of stresses are obtained with the help of construction of a cubic spline over the points where these values are already obtained along one direction having other two fixed. After obtaining the array of points evaluated in such a way, we will map it into other three quarters according to the rules of symmetry inherent to each stress component considered. Thus basing on the initial calculation which has been carried out for $(n \times n \times n) = (n)^3$ points, $(4n \times 4n \times 2n) = 32(n)^3$ points are obtained.

As the result of the carried out calculations and transformations the set $G = \{M_{uvw}(\xi_u, \eta_v, z_w) / -ta \le \xi_u, \eta_v \le ta, -ta \le z_w \le 0\}$ ($u,v = 0..2n$, $w = 0..n$) in points of which the values of stresses $\sigma_{ij}(\xi_u, \eta_v, z_w)$ are known is received.

4.3 Stresses Caused by Tangential Tractions

Calculation of state of stress $\sigma_{ij}^{(\tau)}$ under the action of friction force is also carried out numerically taking advantage of the Cerruti, problem solution $\sigma_{ij}^{(C)}$ [1] used to determine stress components in the half-space caused by unit tangential force:

$$\sigma_{ij}^{(\tau)}(\xi,\eta,z)=\iint\limits_{S(x,y)} q(x,y)\sigma_{ij}^{(C)}(x-\xi,y-\eta,z)dxdy \quad (20)$$

where $q(x,y)$ is the distribution of tangential tractions.
where f – coefficient of friction.

Stick and slip regions are usually considered when rolling friction studied [1]. It is assumed that tangential contact tractions are governed by Coulomb's law $|q(x,y)|=fp(x,y)$ in the slip region and by the law $|q(x,y)|\le fp(x,y)$ in the stick region. In case of elliptic contact the distribution of tangential tractions $q(x,y)$ (Fig. 3) over contact surface to a first approximation can be considered as a superposition of two distributions

$$q'(x,y)=fp_0\sqrt{1-\frac{x^2}{a^2}-\frac{y^2}{b^2}} \text{ and}$$

$$q''(x,y)=-\frac{c}{a}fp_0\sqrt{1-\frac{(x-d)^2}{c^2}-\frac{y^2}{(bc/a)^2}}$$

where f – coefficient of friction, c – a semi-axis of an ellipse of stick region, $d=a-c$.

Thus the problem of finding $q(x,y)$ is reduced to the determination of c that is a separate problem and is not examined in the present paper. In order to determine the state of stress caused by the action of tangential tractions $q(x,y)$ we will assess them by their upper bound taking advantage of Coulomb's law.

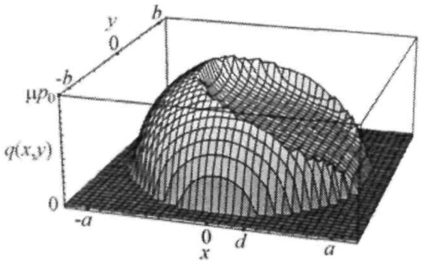

Figure 3. Distribution of tangential contact tractions

Explicit form of expressions (20) is the following [3,4]:

$$\sigma_{xx}^{(\tau)}=\iint\limits_S \frac{fp_0\sqrt{1-\frac{x^2}{a^2}-\frac{y^2}{b^2}}}{2\pi}\left\{-\frac{3(x-\xi)^3}{\rho^5}+(1-2\nu)\left[\frac{(x-\xi)}{\rho^3}-\frac{3(x-\xi)}{\rho(\rho+z)^2}+\frac{(x-\xi)^3}{\rho^3(\rho+z)^2}+\frac{2(x-\xi)^3}{\rho^2(\rho+z)^3}\right]\right\}dxdy, \quad (21)$$

$$\sigma_{yy}^{(\tau)}=\iint\limits_S \frac{fp_0\sqrt{1-\frac{x^2}{a^2}-\frac{y^2}{b^2}}}{2\pi}\left\{-\frac{3(x-\xi)(y-\eta)^2}{\rho^5}+(1-2\nu)\left[\frac{(x-\xi)}{\rho^3}-\frac{(x-\xi)}{\rho(\rho+z)^2}+\frac{(x-\xi)(y-\eta)^2}{\rho^3(\rho+z)^2}+\frac{2(x-\xi)(y-\eta)^2}{\rho^2(\rho+z)^3}\right]\right\}dxdy,$$

$$\sigma_{zz}^{(\tau)}=-\iint\limits_S \frac{3fp_0\sqrt{1-\frac{x^2}{a^2}-\frac{y^2}{b^2}}}{2\pi}\frac{(x-\xi)z^2}{\rho^5}dxdy,$$

$$\sigma_{xy}^{(\tau)}=\iint\limits_S \frac{fp_0\sqrt{1-\frac{x^2}{a^2}-\frac{y^2}{b^2}}}{2\pi}\left\{-\frac{3(x-\xi)^2(y-\eta)}{\rho^5}+(1-2\nu)\left[-\frac{(y-\eta)}{\rho(\rho+z)^2}+\frac{(x-\xi)^2(y-\eta)}{\rho^3(\rho+z)^2}+\frac{2(x-\xi)^2(y-\eta)}{\rho^2(\rho+z)^3}\right]\right\}dxdy,$$

$$\sigma_{xz}^{(\tau)}=-\iint\limits_S \frac{3fp_0\sqrt{1-\frac{x^2}{a^2}-\frac{y^2}{b^2}}}{2\pi}\frac{(x-\xi)^2 z}{\rho^5}dxdy,$$

$$\sigma_{yz}^{(\tau)}=-\iint\limits_S \frac{3fp_0\sqrt{1-\frac{x^2}{a^2}-\frac{y^2}{b^2}}}{2\pi}\frac{(x-\xi)(y-\eta)z}{\rho^5}dxdy,$$

Under rolling with sliding tangential traction for the roller is directed in the positive direction of the x-axis and for the shaft in the negative. Therefore if formulae (21) are used for calculation of stresses in the roller, then in order to calculate stresses in the shaft, expression (21) should be multiplied by (-1).

Calculation of double integrals (21) in each of considered points $M(\xi,\eta,z)$ is performed according to the scheme which was applied to calculation of integrals (19). Values of stresses on the set G are obtained similarly.

4.4 Stresses Caused by Bending and United State of Stress

Stresses

$$\sigma_{ij}^{(b)}=\sigma_{ij}^{(M)}+\sigma_{ij}^{(N)}+\sigma_{ij}^{(Q)} \quad (22)$$

where M, N, Q are internal moment, normal and shear forces in the ring respectively.

The united state of stress for the shaft is obtained by superposition on the set G of calculated stresses $\sigma_{ij}^{(surf)}$, $\sigma_{ij}^{(hs)}$, $\sigma_{ij}^{(\tau)}$, $\sigma_{ij}^{(b)}$:

$$
\begin{aligned}
&\sigma_{ij}(\xi_u,\eta_v,z_w)=\sigma_{ij}^{(n)}(\xi_u,\eta_v,z_w)+\sigma_{ij}^{(\tau)}(\xi_u,\eta_v,z_w)+\\
&+\sigma_{ij}^{(b)}(\xi_u,\eta_v,z_w)=\left[\sigma_{ij}^{(hs)}(\xi_u,\eta_v,z_w)\cup\sigma_{ij}^{(surf)}(\xi_u,\eta_v,0)\right]+\\
&+\sigma_{ij}^{(\tau)}(\xi_u,\eta_v,z_w)+\sigma_{ij}^{(b)}(\xi_u,\eta_v,z_w)=\\
&=\left[\iint_{S(x,y)} p(x,y)\sigma_{ij}^{(B)}(x-\xi_u,y-\eta_v,z)dxdy\cup\sigma_{ij}^{(S)}(\xi_u,\eta_v)\right]+\\
&+\iint_{S(x,y)} fp(x,y)\sigma_{ij}^{(C)}(x-\xi_u,y-\eta_v,z)dxdy+\\
&+\sigma_{ij}^{(M)}(\xi_u,\eta_v,z_w)+\sigma_{ij}^{(N)}(\xi_u,\eta_v,z_w)+\sigma_{ij}^{(Q)}(\xi_u,\eta_v,z_w)
\end{aligned}
\tag{23}
$$

5 CALCULATION RESULTS AND THEIR DISCUSSION

Examples of calculations according to formulae (23) are shown in Fig. 4–8.

During numerical investigation of the state of stress of the considered active system the calculation was carried out for 20x39x39 points in the area $z \in [0; 1{,}5a]$, $x \in [-1{,}5a; 1{,}5a]$, $y \in [-1{,}5a; 1{,}5a]$ under contact load F_N = 500 N. The following values for material properties and geometrical characteristics were used $E_1 = E_2 = 2.01\ 10^{11}$ Pa, $\nu_1 = \nu_2 = 0.3$, R_{11}=0,05 m, friction coefficient f=0.05, R_{12} =0.005 m, R_{21}=0,015 m, $R_{22}=\infty$, thickness and width of a ring: $b = h = 0.006$ m.

The known analytical relationships allow contact stresses along z-axis to be calculated. The values of stresses obtained as the result of the calculations performed along z-axis well correspond to the known solution [1,6]. This confirms the correctness of the used evaluation procedure (Fig. 4 and Tab. 2).

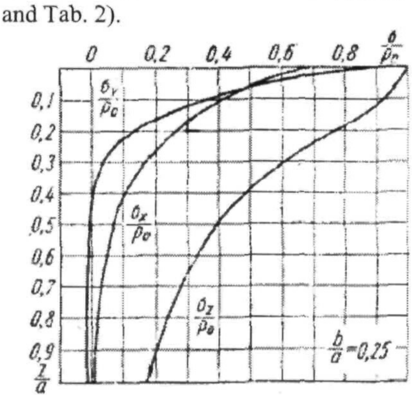

Figure 4. Data available for the stresses along z axis [6]:

Table 2. The result of calculation of contact stresses along z axis caused by normal traction elliptically distributed over the surface of the half-space.

z/a, b/a=0.25	$\sigma_{zz}^{(n)}/p_0$	$\sigma_{xx}^{(n)}/p_0$	$\sigma_{yy}^{(n)}/p_0$
0.	-1.	-0.68	-0.92
0.05	-0.970138	-0.540813	-0.607672
0.1	-0.92384	-0.418952	-0.354803
0.15	-0.850852	-0.32706	-0.202889
0.2	-0.765632	-0.259033	-0.121569
0.25	-0.685324	-0.205577	-0.0698687
0.3	-0.613111	-0.163394	-0.0362213
0.35	-0.548719	-0.130611	-0.0162498
0.4	-0.492018	-0.105067	-0.00493549
0.45	-0.442741	-0.0847497	0.00217467
0.5	-0.39993	-0.0685201	0.00663055
0.55	-0.362521	-0.0555097	0.00922088
0.6	-0.329738	-0.0450548	0.010593
0.65	-0.300905	-0.0365878	0.011283
0.7	-0.275469	-0.0297202	0.0115236
0.75	-0.252927	-0.0241263	0.0114621
0.8	-0.232844	-0.0195523	0.0112062
0.85	-0.21486	-0.0157891	0.0108436
0.9	-0.198866	-0.0127331	0.0104203
0.95	-0.184661	-0.0102676	0.00996822
1.	-0.171426	-0.00811714	0.00950359

The results of calculations for $\sigma_{yy}^{(n)}$ (plane z=0.87a) are given in Fig. 5–8.The analysis of these results allows the following conclusions to be made:

a. According to Fig.5, the distribution of stress tensor component $\sigma_{yy}^{(n)}$ in the volume zone of contact is qualitatively similar for both the roller and the shaft. This corresponds to the usual contact problems concept. However in a quantitative sense the essential decrease (up to ~30 % under conditions of calculation) in the level of contact stresses due to the influence of bending is revealed.

b. According to Fig. 6 the distribution $\sigma_{yy}^{(\tau)}$ is antisymmetric in relation to y-axis. It corresponds to the general idea about the processes of friction. However in a quantitative sense the essential decrease (up to ~15 % under conditions of calculation) of friction force due to the influence of bending is revealed.

c. Fig. 7 illustrates the change of a stress field $\sigma_{yy}^{(n)}$caused by normal contact traction in elements of the system due to the effect of friction force. Such a change has specific features for each of the components of the united state of stress caused by contact load.

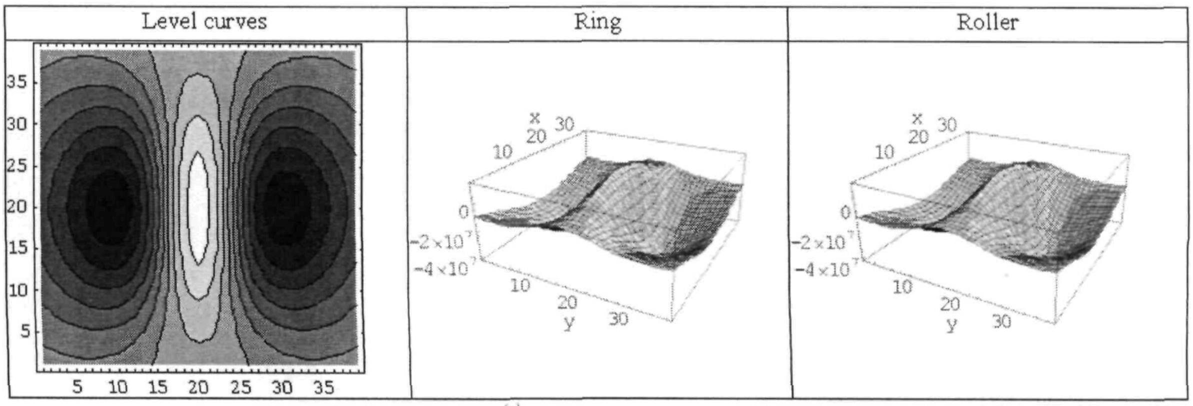

Figure 5. Component $\sigma_{yy}^{(n)}$ of stress tensor caused by normal tractions

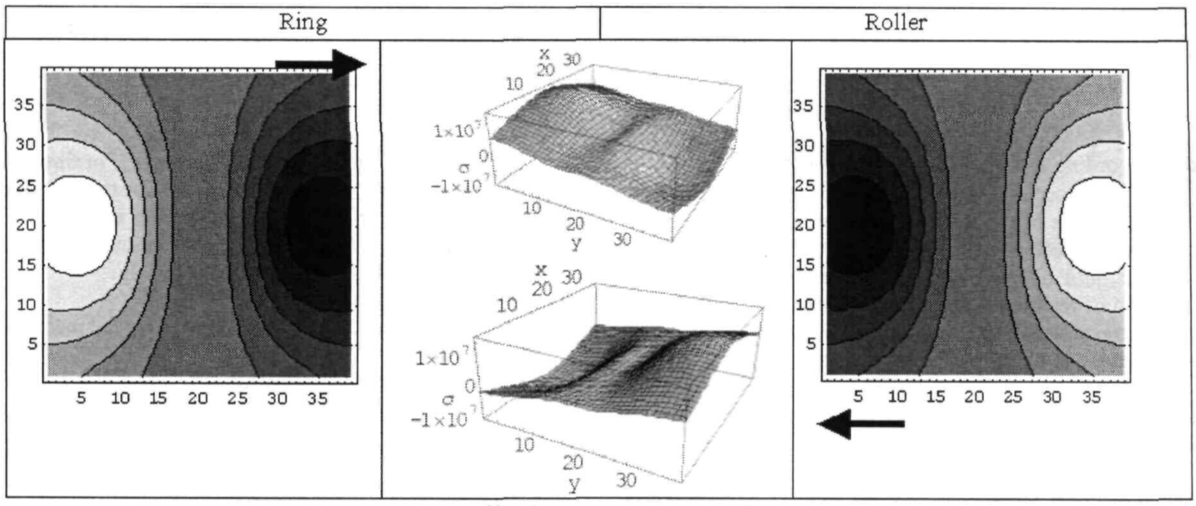

Figure 6. Component $\sigma_{yy}^{(\tau)}$ of stress tensor caused by tangential tractions

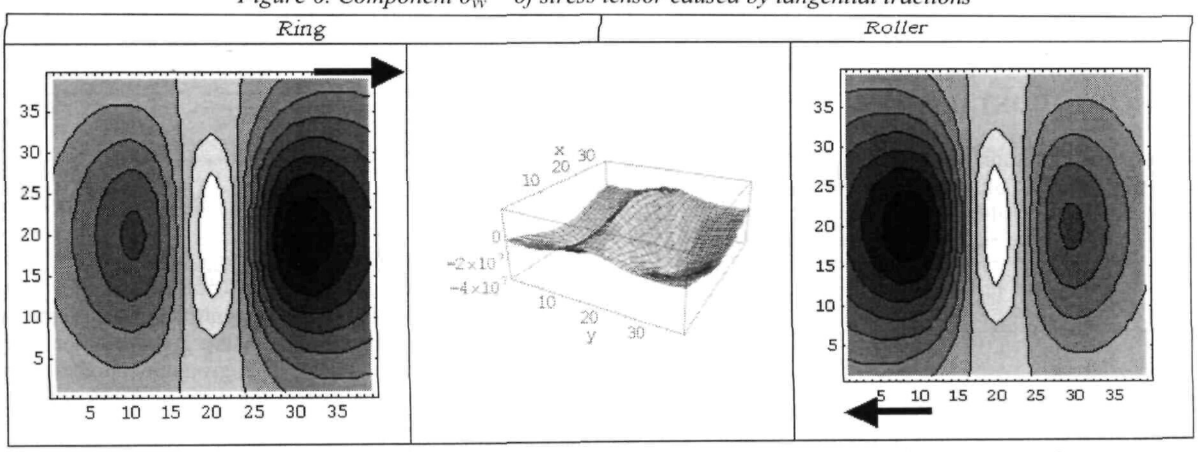

Figure 7. Superposition $\sigma_{yy}^{(n)} + \sigma_{yy}^{(\tau)}$ of components of stress tensors caused by normal and tangential tractions

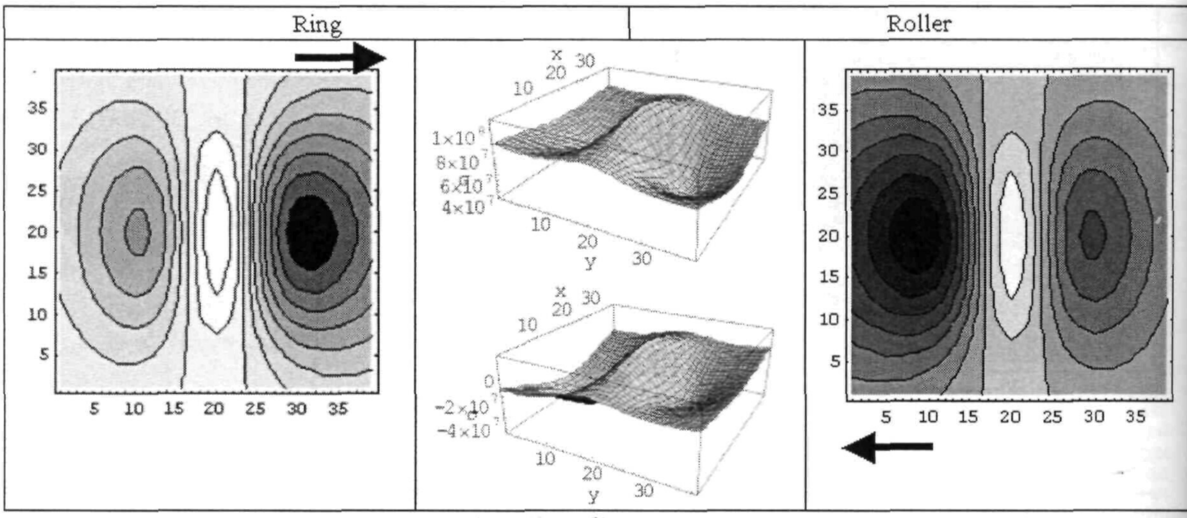

Figure 8. Superposition $\sigma_{yy}^{(n)}+\sigma_{yy}^{(\tau)}+\sigma_{yy}^{(b)}$ of components of stress tensors caused by normal and tangential tractions and bending load

d. According to Fig. 8 (compare with Fig. 7 for $\sigma_{yy}^{(n)}+\sigma_{yy}^{(\tau)}$) effect of stresses caused by bending $\sigma_{yy}^{(b)}$ on the change of the state of stress of the ring is that the signs of effective stresses reverse in certain areas (the field of compressive stresses transforms to the field of tensile stresses). In a quantitative sense such a transformation results in the change of the magnitude of stresses approximately up to 80 MPa.

Conclusions 1-3 are similar for the other components of stress tensor.

Thus, formulae (13), (15), (18), (20), (22), (23) give the procedures of an exhaustive analysis of the stressed state in the neighborhood of an elliptic non-conforming contact of active system elements

6 DYNAMIC CONTACT

The obtained solution allows dynamic contact provided that the change of contact parameters in time is established to be analyzed.

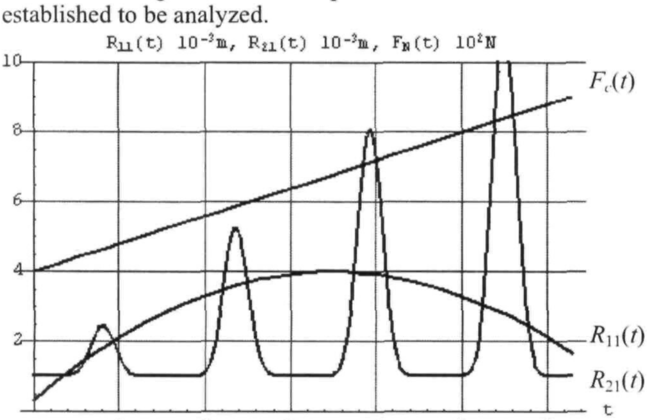

Figure 9. Law of change R_{11}, R_{21} u F_c

If, for instance, we change R_{11}, R_{21} and F_c in time, as it is shown in Fig. 9, then the change of contact parameters, according to formulae (9), is as shown in Fig. 10. Here X_{ab}, Y_{ab} are the magnitudes of semi-axes of the contact ellipse along the axes x and y respectively.

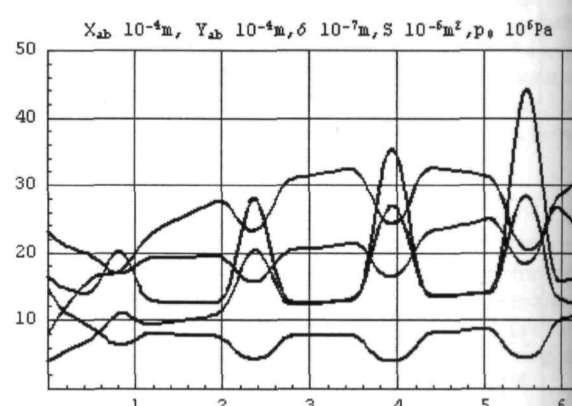

Figure 10. Change X_{ab}, Y_{ab}, S, p_0 and δ in time

The distributions of stresses σ_{zz} and σ_{xz} in the discrete moments of time in planes z=0.5a (the top pair) y=0 (the bottom pair) where a – the magnitude of the greater semi-axis of the contact ellipse at the given moment of time are shown in Fig. 11-14. Each group of four figures gives the exhaustive analysis of the state of stress at the given moment of time.

The analysis of Fig.11-14 and Fig. 9-10 shows that the developed model allows to describe correctly the change of the shape and magnitude of stresses distribution as the result of time change of bodies geometry in the contact area and the applied load (Fig. 9) through the change of contact area parameters (Fig. 10).

In conditions of calculation the planes to which radii R_{11} and R_{21} belong are parallel to axes y and x respectively. Consider Fig. 11 and 13 and corresponding points t=0 and t=4 in Fig. 9 and 10. It is evident that at $R_{11}>R_{21}$ (Fig. 9) the greater semi-axis of the contact ellipse is oriented along y-axis (as well as the distribution of stresses in Fig. 11) i.e. $Y_{ab}>X_{ab}$. As this takes place the magnitude of stresses at a point t=0 is greater than at a point t=4 because $S(1)<S(4)$ and $p_0(1)>p_0(4)$. The relations inverse to the described ones take place in the moments of time t=2 and t=6.

The analysis for other moments of time and components of stress tensor is carried out similarly.

7 CONCLUSION

The following problems have been set up and solved when developing the method of investigation of the state of stress of the simplest model of wheel/rail system designed as the roller/ring system:

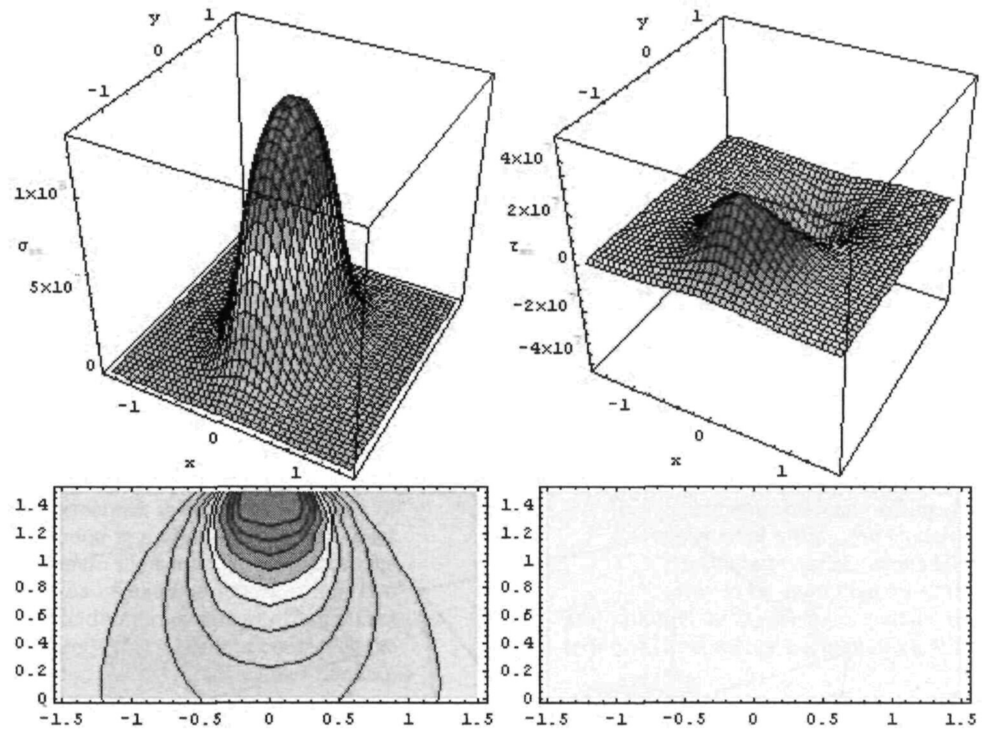

Figure 11. Distribution of stresses $\sigma_{zz}^{(n)}$ and $\sigma_{xz}^{(n)}$ in the initial moment of time (t=0)

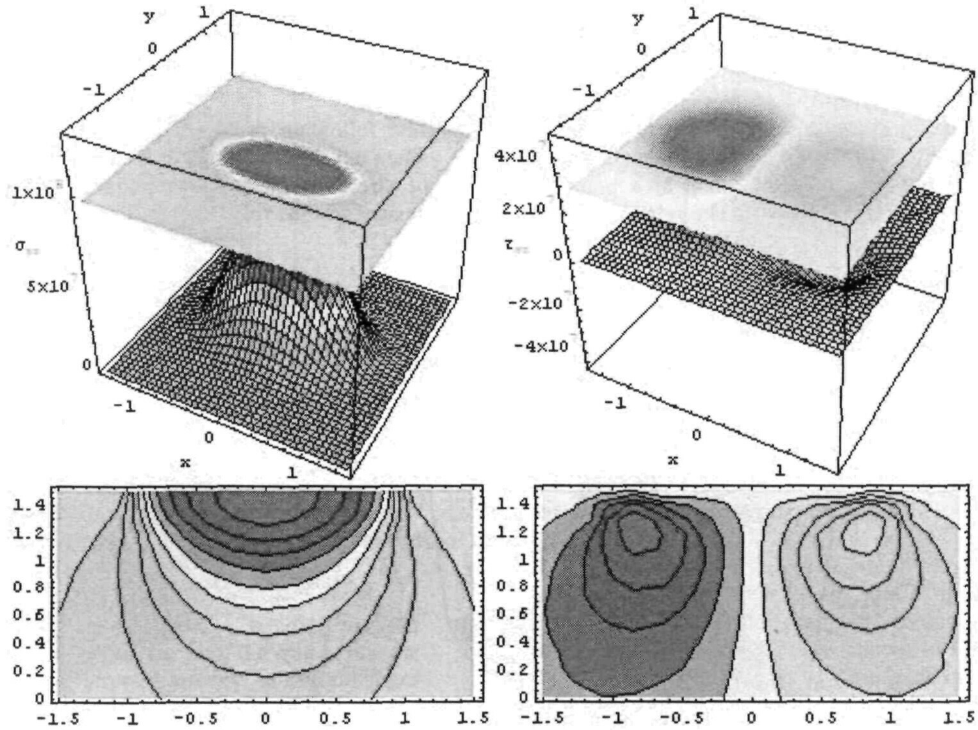

Figure 12. Distribution of stresses $\sigma_{zz}^{(n)}$ and $\sigma_{xz}^{(n)}$ in the moment of time t=2

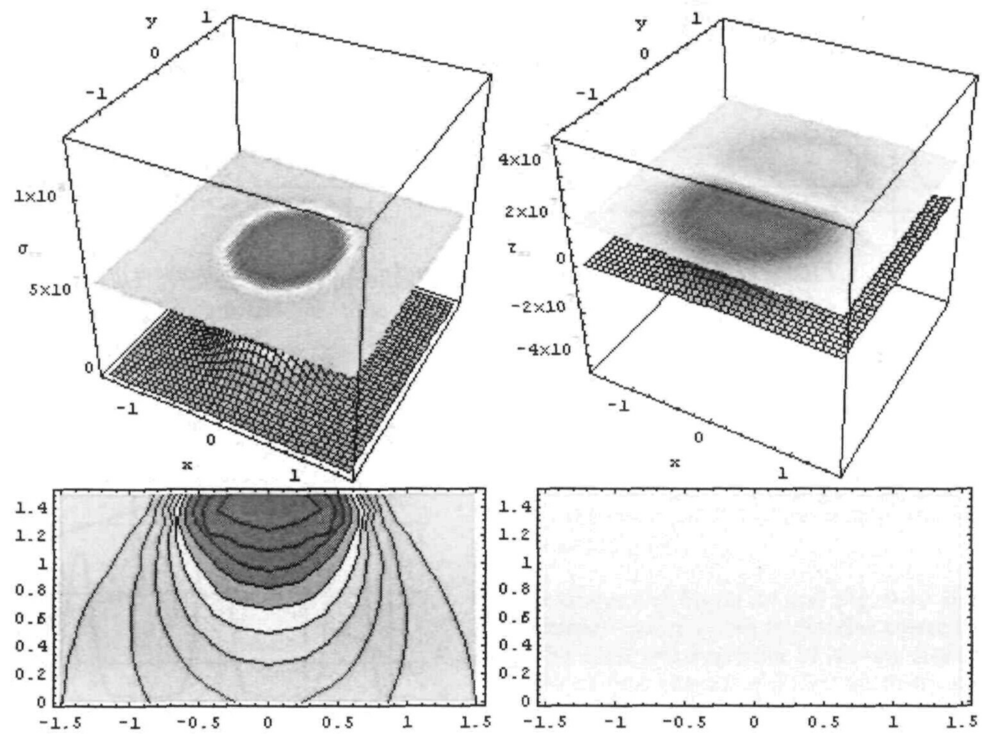

Figure 13. Distribution of stresses $\sigma_{zz}^{(n)}$ and $\sigma_{xz}^{(n)}$ in the moment of time t=4

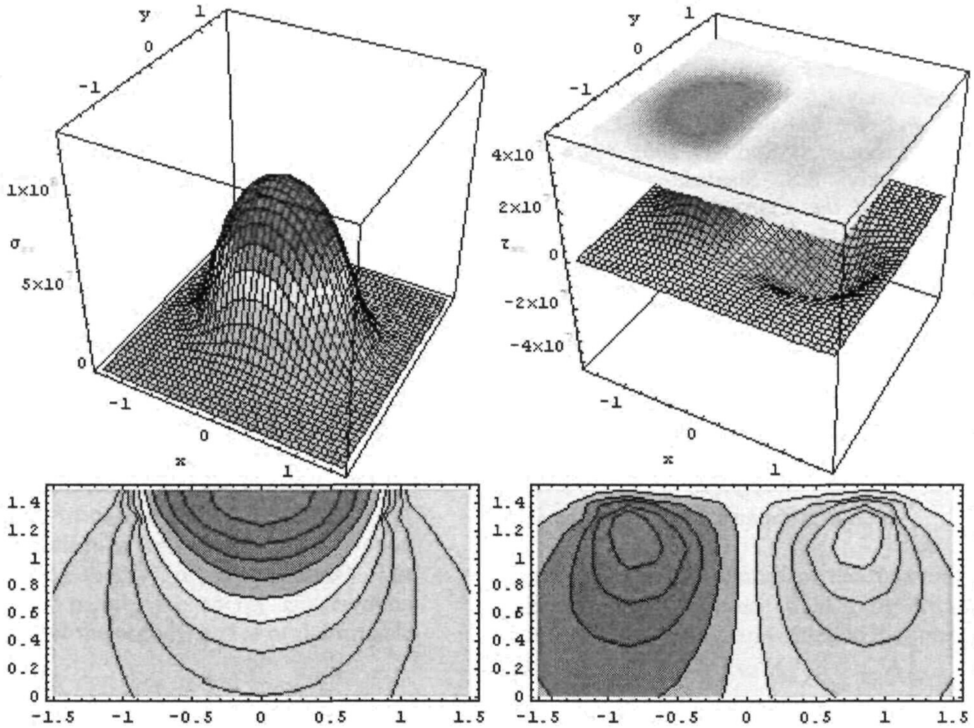

Figure 14. Distribution of stresses $\sigma_{zz}^{(n)}$ and $\sigma_{xz}^{(n)}$ in the moment of time t=6

1. The system of principles is stated as the basis of the problem solution regarding the state of stress of roller/ring system elements. In particular, the scheme of division of external load F_N into two components applied to the system is offered. One component is observed at a point of contact of the roller and the ring and the other causes bending of the ring.
2. When solving the contact problem:
   - the change of contact parameters due to bending of the ring is taken into account.
   - the full pattern of stresses distribution in the volume zone of contact caused by the effect of normal and tangential tractions elliptically distributed over the contact surface is obtained; simplified formulae (16) for calculation of stresses on the contact surface are introduced; integrals (19) and (21) for determination of all the components of stress tensor under the contact surface are recorded,
   - numerical methods including Simpson formula, construction and integration of the cubic spline are used in order to conduct integration in formulae (19) and (21),
   - on the basis of the obtained regular grid the following procedures are developed:
     a. Interpolation for calculation of stresses in the points inside the grid;
     b. Symmetric mapping of array of points calculated for the quarter of a considered volume, which allowed data array to be multiplied by 32 times.
3. The solution of a dynamic contact problem in terms of Hertz theory assumptions is given.

The solution of the problem of the state of stress of roller/ring system elements presents a general view in a sense that the method of the calculation of the stresses caused by both surface and volume deformation is given. Naturally there arises the problem of realization of the similar method for the real wheel/rail system. In our opinion, it is possible with the account of all the variety of fields of stresses (including residual) caused by spatial system of cyclic loads. And though computing difficulties will undoubtedly arise here, this specific target now seems quite tractable.

The general conclusion is the following: ignoring bending stresses while analyzing the state of stress of the roller/shaft system only with the account of contact loading can result in the distorted idea about the state of stress of the system elements and hence in the incorrect estimation of its serviceability. This concept corresponds to the main ideas of tribo-fatigue [2] confirmed experimentally.

REFERENCES

[1] K. L. Johnson: *Contact Mechanics*, Cambridge University Press, Cambridge, 1985, 453 pp.

[2] L.A. Sosnovskiy: *Tribo-Fatigue. Wear-fatigue damage and its prediction (Foundations of engineering mechanics)*, Springer, 2005, 424 pp.

[3] L.A. Sosnovskiy, S.S. Sherbakov: *About the Classification of the Contact Problems for the Active Systems of Machines* (in Russian)// *Modern Methods of Machines Design. Calculation, Construction, Technology. Proc. of the II International Scientific and Technical Conference* (Minsk, Belarus, December 6-10, 2004), Vol. 4, BNTU, Minsk, 2004, pp 46-57.

[4] L.A. Sosnovskiy, V.I. Senko, S.S. Sherbakov, N.A. Zalessky: *Study of the State of Stress of the Simplest Model of Wheel/Rail System* (in Russian). *Vestnik BelGUTa: Nauka i transport*, 2005, vol. 2, 18-41 pp.

[5] S.S. Sherbakov: *Study of the State of Stress of Active System for Mechano-Rolling Fatigue Tests// Dynamics, Durability and Reliability of Agricultural Machines. Proc. of the I International Scientific and Technical Conference* (in Russian), (Ternopil, Ukraine, October 4-7, 2004), TSTU, Ternopil, 2004, pp 400-407.

[6] S.D. Ponomaryev et al: *Strength Calculations in Machine-Building* (in Russian), vol. 2, State Scientific and Technical Publishing House of Machine-Building Literature, Moscow, 1958, pp 386-486.